AGU PUBLICATIONS

Geophysical Research Letters

RESEARCH LETTER

10.1002/2017GL076433

Key Points:

- Sea ice losses confined to the Atlantic or Pacific sector of the Arctic have opposite effects on the winter stratospheric polar vortex
- Tropospheric Arctic Oscillation response is dependent on the sea ice loss region (Atlantic or Pacific sector of the Arctic) and magnitude
- Broader Arctic Oscillation-induced midlatitude surface temperature response is modulated by the local influence of the sea ice loss region

Supporting Information:

- Supporting Information S1

Correspondence to:
C. M. McKenna,
christine.mckenna@bas.ac.uk

Citation:
McKenna, C. M., Bracegirdle, T. J., Shuckburgh, E. F., Haynes, P. H., & Joshi, M. M. (2018). Arctic sea ice loss in different regions leads to contrasting Northern Hemisphere impacts. *Geophysical Research Letters*, *45*, 945–954. https://doi.org/10.1002/2017GL076433

Received 18 AUG 2017
Accepted 15 DEC 2017
Accepted article online 21 DEC 2017
Published online 19 JAN 2018

Arctic Sea Ice Loss in Different Regions Leads to Contrasting Northern Hemisphere Impacts

Christine M. McKenna[1,2], Thomas J. Bracegirdle[1], Emily F. Shuckburgh[1], Peter H. Haynes[2], and Manoj M. Joshi[3,4]

[1]British Antarctic Survey, Cambridge, UK, [2]Department of Applied Mathematics and Theoretical Physics, University of Cambridge, Cambridge, UK, [3]Centre for Ocean and Atmospheric Sciences, University of East Anglia, Norwich, UK, [4]Climatic Research Unit, University of East Anglia, Norwich, UK

Abstract To explore the mechanisms linking Arctic sea ice loss to changes in midlatitude surface temperatures, we conduct idealized modeling experiments using an intermediate general circulation model and with sea ice loss confined to the Atlantic or Pacific sectors of the Arctic (Barents-Kara or Chukchi-Bering Seas). Extending previous findings, there are opposite effects on the winter stratospheric polar vortex for both large-magnitude (late 21st century) and moderate-magnitude sea ice loss. Accordingly, there are opposite tropospheric Arctic Oscillation (AO) responses for moderate-magnitude sea ice loss. However, there are similar strength negative AO responses for large-magnitude sea ice loss, suggesting that tropospheric mechanisms become relatively more important than stratospheric mechanisms as the sea ice loss magnitude increases. The midlatitude surface temperature response for each loss region and magnitude can be understood as the combination of an “indirect” part induced by the large-scale circulation (AO) response, and a residual “direct” part that is local to the loss region.

1. Introduction

Since 1979, Arctic sea ice extent has declined in all months and, in particular, by more than 13% per decade in September (National Snow and Ice Data Center, 2016). This has contributed to enhanced near-surface warming in the Arctic, which has occurred at double the rate of lower latitudes since 1989 (Screen & Simmonds, 2010). In contrast, this decline has coincided with an apparent increase in severe winter weather across some midlatitude regions (Cohen et al., 2014), including central Eurasia where average winter surface air temperatures have reduced by 1.25°C over the past 25 years (McCusker et al., 2016). There have also been recent unusually cold and snowy winters observed in 2009–2010 and 2010–2011 across parts of Europe (Guirguis et al., 2011; Osborn, 2011), and in 2013–2014 across parts of North America (Van Oldenborgh et al., 2015).

The simultaneous occurrence of recent Arctic sea ice loss and apparent increases in severe midlatitude winters has led to much research into the mechanisms that could explain a link. It has been suggested that sea ice loss excites the negative phase of the Arctic Oscillation/North Atlantic Oscillation (AO/NAO) (which is linked to colder conditions in key regions of midlatitudes) through tropospheric eddy feedbacks (Deser et al., 2004; Honda et al., 2009; Seierstad & Bader, 2009), or a weakening of the stratospheric polar vortex and the resulting effect on the troposphere (García-Serrano et al., 2015; Kim et al., 2014; King et al., 2016; Nakamura et al., 2015; Peings & Magnusdottir, 2014), or a combination of both (Nakamura, Yamazaki, Honda, et al., 2016; Wu and Smith, 2016). It has also been suggested that sea ice loss modifies tropospheric stationary Rossby wave propagation, which leads to a stronger Siberian High and therefore stronger cold air advection over Eurasia (Honda et al., 2009; Mori et al., 2014; Petoukhov & Semenov, 2010).

However, these mechanisms remain uncertain because it is difficult to disentangle the complex web of potential processes involved (Overland et al., 2016), there are high levels of natural atmospheric variability (McCusker et al., 2016; Screen et al., 2013), and model results are contrasting—for example, some studies find a positive AO/NAO response (Orsolini et al., 2012; Screen et al., 2014), no significant AO/NAO response (Boland et al., 2016; Screen et al., 2013; Singarayer et al., 2006), or a stronger polar vortex (Cai et al., 2012; Scinocca et al., 2009; Screen et al., 2013; Sun et al., 2014). Here we make understanding these mechanisms more tractable by conducting idealized modeling experiments.

To address the issues of complexity and statistical robustness, we use an intermediate general circulation model (GCM). Such models are useful because they are complex enough to simulate a variety of important processes, but are relatively simple and computationally fast compared to state-of-the-art GCMs. This helps to disentangle different processes from one another and allows for long simulations, making a statistically robust response more attainable.

In terms of understanding the contrasting results of previous studies, we first investigate whether the contrasting stratospheric responses can be explained by the different spatial patterns of sea ice loss that were assumed. This was examined previously by Sun et al. (2015) (hereafter SDT15), who found that when sea ice loss is mainly confined to the Atlantic sector of the Arctic (in their case the Barents-Kara, Greenland, and Labrador Seas), the polar vortex weakens in winter; if it is mainly confined to the Pacific sector (in their case the Bering and Okhotsk Seas), the vortex strengthens. Their explanation is that the anomalous stationary Rossby waves generated in the Atlantic (Pacific) case constructively (destructively) interfere with climatological stationary Rossby waves, which enhances (suppresses) upward wave propagation into the stratosphere and decelerates (accelerates) the stratospheric flow. This contrast in interference occurs because the climatological waves are fixed in phase — since they are generated by fixed orography and land-sea thermal contrasts — but the phase of the anomalous waves depends on the longitude of the sea ice loss. Smith et al. (2010) previously argued for similar effects of varying longitudinal positions of snow cover anomalies.

Two remaining questions that we address are whether different spatial patterns of sea ice loss can also explain the contrasting tropospheric responses in previous studies, and what effects different loss regions have on midlatitude surface temperatures. Since Baldwin and Dunkerton (2001) and many subsequent studies find that a weaker (stronger) polar vortex is often followed by a negative (positive) tropospheric AO/NAO, in studies with more Atlantic (Pacific) sector sea ice loss, we might expect a negative (positive) AO/NAO — indeed, this is the case in Kim et al. (2014) (Cai et al., 2012) — and colder (warmer) regions in midlatitudes. However, while SDT15 find that the zonal mean tropospheric eddy-driven jet shifts south (a negative AO) for their Atlantic experiment, they find no shift for their Pacific experiment. They also do not examine the surface temperature response in the separate Atlantic and Pacific cases. Therefore, we look in detail at stratosphere-troposphere interactions and the surface temperature response in each case. Other studies examine the tropospheric and surface temperature response to regional sea ice anomalies, but do not focus on the role of the stratosphere (Alexander et al., 2004; Koenigk et al., 2016; Pedersen et al., 2016; Screen, 2017a).

In summary, here we conduct idealized modeling experiments using an intermediate GCM to investigate the following questions:

1. Do sea ice losses confined to the Atlantic or Pacific sector of the Arctic have opposite effects on the stratospheric polar vortex?
2. Are there corresponding opposite effects on the tropospheric AO?
3. What are the effects on midlatitude surface temperatures?

2. Method

2.1. Numerical Model

We use the spectral primitive equation atmospheric model, IGCM4 (Intermediate Global Circulation Model, version 4; Joshi et al., 2015), with a horizontal resolution of T42 (~2.8°) and 35 vertical sigma levels. These levels extend from the surface up to approximately 0.1 hPa (~65 km), with 13 levels in the stratosphere. Since the model is atmosphere-only, climatological monthly mean surface temperatures (T_s) are prescribed over the ocean. There is no explicit sea ice field, but its important effects (e.g., albedo) are parameterized through the T_s field. The T_s over land is computed from the surface fluxes at each time step. All the main greenhouse gases are generally prescribed using climatological data, and moist processes are parameterized in a simplified manner.

The model's zonal mean zonal wind climatology compares well with ERA-40 reanalysis data in both the troposphere and stratosphere (Joshi et al., 2015). O'Callaghan et al. (2014) show that stratospheric sudden warmings in IGCM4 are realistic in terms of frequency, type, and the strength of subsequent stratosphere-troposphere coupling. Climatological stationary waves that propagate into the stratosphere in winter (wave-1/2/3) are weaker in IGCM4 than in ERA-Interim reanalysis data, but are similar in phase. For further details on IGCM4, see Joshi et al. (2015).

2.2. Experiments

Three main experiments — one control run and two perturbation runs — were conducted, each of which consists of a 1 year spin-up followed by another 200 years. The spin-up year is discarded in the results. In the control run (CTL) we prescribe an annually repeating cycle of historical monthly mean T_s over the ocean using ERA-Interim reanalysis data (Dee et al., 2011) averaged over 1979–2014. In the Atlantic/Pacific sector perturbation run (ATL/PAC), the same boundary conditions are used as in CTL, but with an annually repeating cycle of monthly mean T_s anomalies added in the Barents-Kara/Chukchi-Bering Seas representing late 21st century sea ice retreat. Our anomalies are more regionally confined than SDT15's to allow a clean comparison of the effects of sea ice loss in the Atlantic versus Pacific sectors and the mechanisms involved. The Barents-Kara and Chukchi-Bering Seas were chosen because it is in these regions that projections of surface temperature appear most diverse across the CMIP5 (Coupled Model Intercomparison Project Phase 5; Taylor et al., 2012) models (Figure S1 in the supporting information).

Figures S2a and S3a show the ocean T_s in each run and T_s anomalies for ATL and PAC (see Text S2 for details on how the anomalies were derived). The anomalies emerge in October, peak in December/January, then reduce going into spring. The resulting anomalous upward surface heat fluxes peak at ~240 W/m^2 in winter (Figures S2b and S3b), while SDT15's peak at ~250 W/m^2, showing that our anomalous forcing is comparable in magnitude.

We examine the linearity of the key results in ATL and PAC by conducting two further perturbation runs (0.5ATL and 0.5PAC) with half the magnitude of imposed T_s anomalies (Figures S4a and S5a). This is important to understand because the CMIP5 models project different magnitudes of Arctic warming (Figure S1), and only a few studies have compared the responses to different sea ice loss magnitudes (e.g., Petoukhov & Semenov, 2010; Peings & Magnusdottir, 2014). The 0.5ATL and 0.5PAC runs were conducted for 300 years, since for a smaller forcing a longer run is required to achieve statistical significance. When analyzing these runs we used an extended 300 year long version of CTL.

2.3. Data Analysis

We define the response of any field by its difference between the perturbation run and control run (e.g., ATL–CTL). We show November–February for ATL/0.5ATL and November–January for PAC/0.5PAC, because this is when the large-scale atmospheric response is statistically significant (hereafter "significant") in each run. This reflects when the imposed T_s anomalies and anomalous surface heat fluxes (Figures S2–S5) are strongest (these are quite weak in February in PAC/0.5PAC). In all figures stippling indicates a two-sided t test 95% confidence level, unless otherwise stated (see Text S3 for details).

3. Results

3.1. Stratospheric Response

In the ATL/PAC runs the stratospheric polar vortex is significantly weaker/stronger in November–February/November–December than in CTL (Figure 1a). Plots of the Eliassen-Palm (EP-flux) and its divergence (Figure S6a) show that this is consistent with an enhancement/suppression of upward Rossby wave propagation in November–December around the latitudinal range of the imposed T_s anomalies (~60°N–80°N). Decomposing the EP flux into its zonal wave-1/2/3 components shows that wave-1 waves explain most of these changes (not shown). Indeed, if we examine the wave-1 component of geopotential height (Z) averaged over 60°N–80°N and November–December, this enhancement/suppression appears to be due to constructive/destructive linear interference between anomalous and climatological wave-1 stationary waves (Figure S6b). The westward tilt of the waves with height indicates that they are vertically propagating, and the amplitude of the waves naturally increases with height because of decreasing density.

Note that the total anomalous vertical wave propagation is in fact composed of the previously described time-mean linear (TM_{LIN}) component as well as a time-mean nonlinear (TM_{NLIN}) component, and high-frequency wave fluctuation (FL) component (Smith et al. (2010); see Text S5 for details). However, we find that TM_{LIN} does indeed dominate in both ATL and PAC (see Figure S7). Sun et al. (2015) use a different decomposition method (Nishii et al., 2009), but the results of this method are more difficult to interpret since it mixes the FL component in with the other terms. As such, this method is more suitable for observational data records, which are often limited in time. Smith et al.'s (2010) method is more suitable for long model experiments, since they allow fluctuations about the time-mean to be more easily extracted. Regardless,

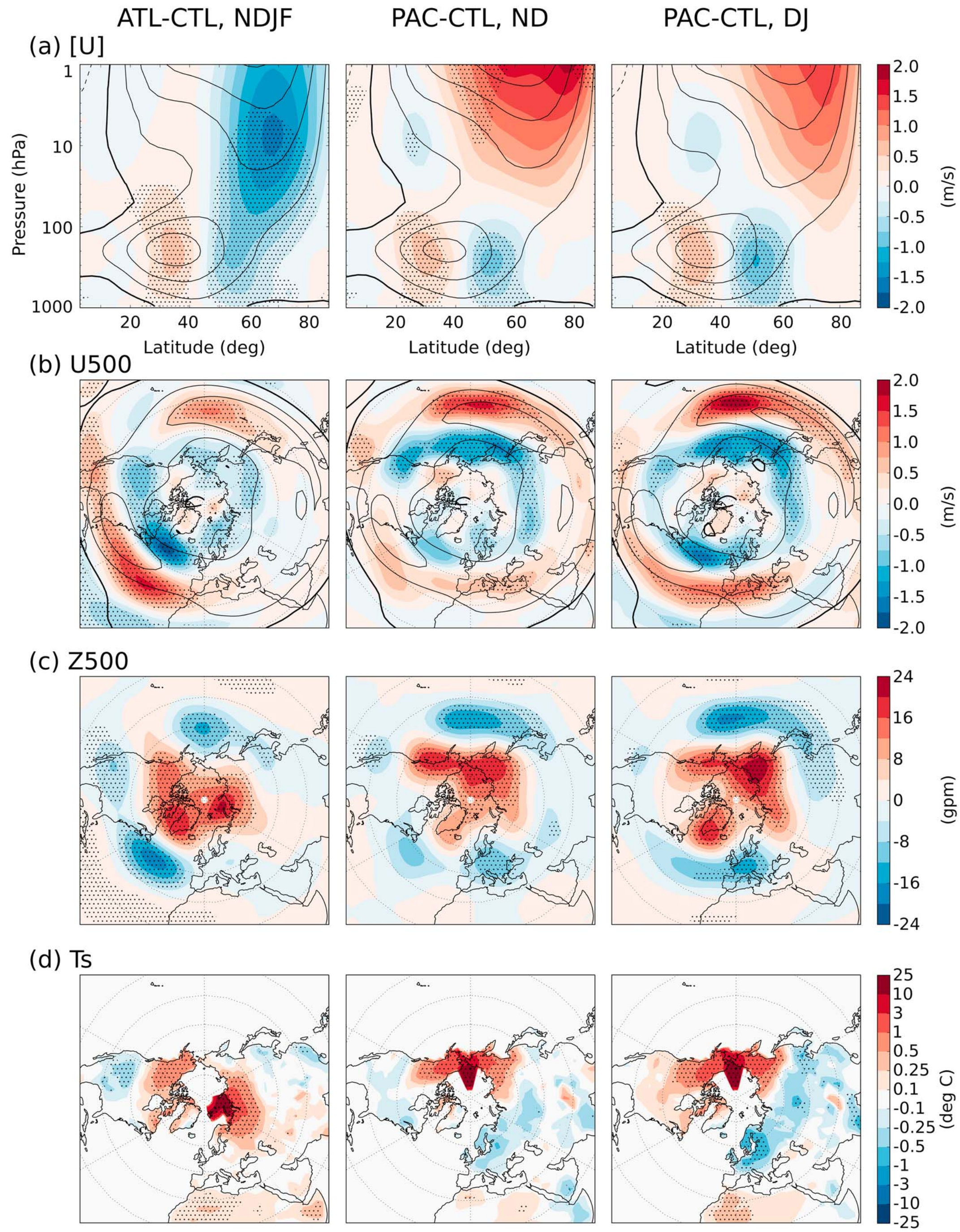

Figure 1. Response (shading) of (a) zonal mean zonal wind, (b) 500 hPa zonal wind, (c) 500 hPa geopotential height, and (d) surface temperature, in (left) ATL NDJF, (middle) PAC ND, and (right) PAC DJ. Contours show climatological values from control run CTL (interval: 10 m/s) and stippling indicates a significant response at a 95% confidence level.

we also found that the linear component dominated using the Nishii et al. (2009) decomposition, in agreement with Sun et al. (2015).

Focusing now on 0.5ATL/0.5PAC, the polar vortex is weaker/stronger in November–February/November–January than in CTL (Figure S8a) consistent with ATL/PAC. The responses are not significant, but the vortex is significantly stronger in 0.5PAC than in 0.5ATL (Figure S9a). The response is linear in 0.5PAC but nonlinear (too weak) in 0.5ATL, which may partly reflect the nonlinear surface heat flux anomalies in 0.5ATL (compare Figures S2b and S4b). However, the heat flux anomalies in 0.5PAC are also nonlinear (Figures S3b and S5b).

Further plots (not shown) are mostly consistent with ATL and PAC, but in both 0.5ATL and 0.5PAC there are limited regions of significance in the stratospheric EP flux divergence and 60°N–80°N wave-1 Z. As in ATL and PAC, the time-mean linear component of the zonal mean eddy heat flux response explains a large part of the anomalous vertical wave propagation in 0.5ATL and 0.5PAC.

3.2. Tropospheric Response

While there are opposite stratospheric responses in the ATL and PAC runs, the tropospheric responses both resemble a similar strength negative AO. This is shown in Figures 1a–1c by the response in zonal mean zonal wind (an equatorward shift of the zonal mean eddy-driven jet), the 500 hPa zonal wind (an equatorward shift of the Atlantic eddy-driven jet and strengthening of the Pacific eddy-driven jet as in Ambaum et al. (2001)), and the 500 hPa geopotential height, Z500 (positive/negative heights at higher/lower latitudes). Indeed, projecting the November–February/November–January Z500 response in ATL/PAC onto the November–February AO from CTL (using linear least squares regression) shows that the AO explains 66%/75% of its spatial variance.

In 0.5ATL/0.5PAC, the tropospheric responses resemble a negative/positive AO (Figures S8a–S8c), which is consistent with the weaker/stronger polar vortex and agrees/disagrees with ATL/PAC. Figure S9 highlights that there are significant stratospheric differences between ATL and PAC, and between 0.5ATL and 0.5PAC, but only in the latter case are there corresponding significant differences in the tropospheric AO.

3.3. Surface Response

While the tropospheric circulation response resembles a negative AO in both the ATL and PAC runs, there are contrasts between ATL and PAC in the T_s response (Figure 1d). Specifically, while a negative AO is associated with Northern European cooling, this only occurs in PAC, and in ATL there is no evidence of this. Additionally, a negative AO is associated with cooling in eastern North America, but this does not occur in PAC, and in ATL cooling only occurs in western North America.

To understand this, we decompose the T_s response into an "indirect" part and a "direct" part. This is done by extending the approach of Deser et al. (2004), who decompose the circulation response into an indirect part and a direct part, where the former is defined as the part that projects onto the model's leading mode of internal variability (i.e., the large-scale AO-like part generated indirectly through tropospheric nonlinear eddy feedbacks), and the latter is defined as the residual (the full minus indirect circulation response).

Specifically, we define the indirect T_s response as the part induced by the indirect circulation response (although further leading modes of variability are used here, as explained shortly). To compute this part, we first find the indirect circulation response by projecting the Z500 response onto the leading empirical orthogonal functions (EOFs) from CTL. The EOFs are defined at 500 hPa as in Deser et al. (2004), since Z may be influenced by boundary layer and orographic effects near the surface, and we are interested in large-scale changes. We then extend Deser et al.'s (2004) approach and temporally regress the normalized principal components (PCs) associated with each EOF onto T_s in CTL. This gives a map of the indirect T_s response for each EOF for a PC value of 1. The maps are then scaled by the regression coefficients obtained for each EOF in the Z500 projections. To calculate the significance of the indirect T_s response we use a two-sided 95% confidence interval obtained from the PC-T_s regressions.

In terms of the direct T_s response, we define this as the residual (the full minus indirect T_s response), similar to Deser et al.'s (2004) definition of the direct circulation response. While the direct T_s response is related to the direct circulation response, the former is also influenced by other factors (e.g., the interaction of climatological winds with the imposed T_s anomalies). They should be similar, however, in terms of being local to the sea ice loss region. Hence, for the Z500 projections we use the first three EOFs, since only projecting onto EOF1 (the AO) gave a Z500 residual containing EOF2 (the Pacific-North American pattern) in ATL and PAC, and EOF3 (a dipole between the North Atlantic and North Pacific) in ATL. The significance of the direct T_s response is calculated by finding the residual response in each year and applying a t test as described in Text S3.

Figure 2 shows the indirect and direct parts of the T_s and Z500 responses in ATL and PAC. Only the EOF1-induced indirect T_s response is shown, since the EOF2-induced and EOF3-induced responses are small. Focusing first on the indirect T_s response, notice it is large scale in both ATL and PAC, as expected from the large-scale nature of the AO. The most notable features are a cooling in eastern North America and Northern Europe, the latter of which explains a large part of the Northern European cooling in the full PAC response. Moving onto the direct T_s response, notice that it and the related direct Z500 response are indeed relatively local to the loss region in both ATL and PAC. Furthermore, it is encouraging that the direct Z500 response

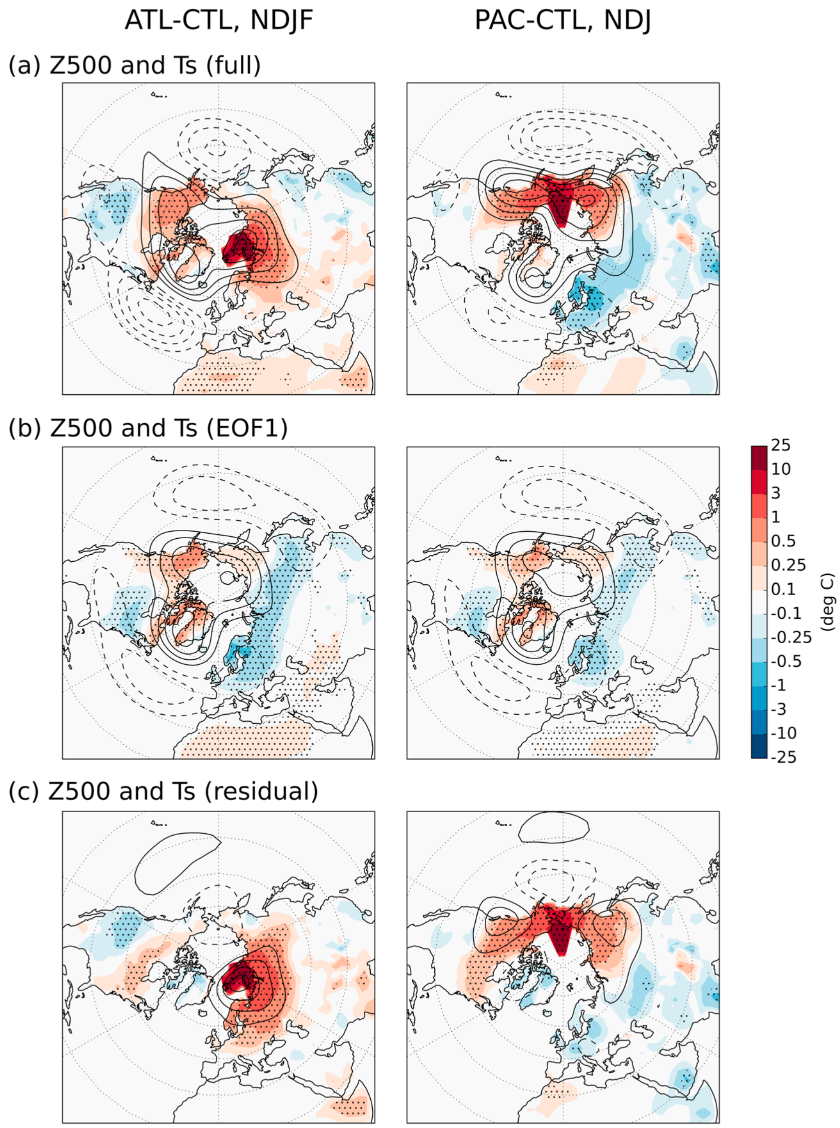

Figure 2. Response of surface temperature (shading) and 500 hPa geopotential height (contours; interval: 4 gpm) in (left) ATL NDJF and (right) PAC NDJ. (a) Full response, (b) indirect part due to EOF1 (the AO), and (c) direct part (residual). Stippling indicates a significant surface temperature response at a 95% confidence level.

becomes more anticyclonic with height above the forcing (cyclonic near the surface — not shown — to anticyclonic (less cyclonic) at 500 hPa in ATL (PAC)) as predicted by linear theory (Hoskins & Karoly, 1981). In ATL, the anticyclone above the forcing is consistent with advection of anomalously warm air from the Barents-Kara Seas to Northern Europe and the counteraction of AO-induced cooling there. Additionally, the direct Z500 anomalies downstream of the forcing may induce the dipole in direct T_s anomalies over North America, which counteract AO-induced eastern North American cooling and explain the western North American cooling in the full response. In PAC, the high over western North America and low north of Hudson Bay in the direct Z500 response are consistent with advection of anomalously warm air from the Chukchi-Bering Seas to eastern North America and the counteraction of AO-induced cooling there. However, note that there is residual cooling in Northern Europe. This may be associated with the residual low; indeed, the NAO low center appears eastward shifted in the full Z500 response (similar to the findings of Pedersen et al. (2016)) — a pattern not captured by the EOFs used in the projections.

The T_s responses are not decomposed for 0.5ATL and 0.5PAC since they have limited significance. However, in November–February in 0.5ATL (December–January in 0.5PAC) there is cooling (significant warming) in eastern North America and no cooling (nonsignificant warming) in Northern Europe, consistent with the negative (positive) AO and a direct warming effect local to the loss region (Figure S8d).

4. Discussion and Conclusions

The research questions from section 1 will now be addressed, which broadly aim to improve understanding of the mechanisms that may link Arctic sea ice loss to changes in midlatitude surface temperatures. A schematic summarizing the proposed key mechanisms is shown in Figure 3.

With respect to the first research question (Do sea ice losses confined to the Atlantic or Pacific sector of the Arctic have opposite effects on the stratospheric polar vortex?), in our model experiments Atlantic sector (Barents-Kara Seas) and Pacific sector (Chukchi-Bering Seas) sea ice loss do have opposite effects on the stratospheric polar vortex. Specifically, in the Atlantic/Pacific case the vortex weakens/strengthens in November–February/November–January due to enhanced/suppressed upward Rossby wave propagation (indicated respectively in Figure 3 by the gray arrows and vortex thickness, and black wavy arrows). This enhancement/suppression is due to constructive/destructive linear interference between anomalous and climatological stationary Rossby waves (indicated in Figure 3 by the relative phase of the red and gray wavy arrows). These results hold for both large-magnitude (late 21st century) and moderate-magnitude sea ice loss and, therefore, our results extend the generality of SDT15's finding that different spatial patterns of (large-magnitude) sea ice loss can explain the contrasting stratospheric responses in previous studies.

Now we address the second research question (Are there corresponding opposite effects on the tropospheric AO?). We find that Atlantic or Pacific sector sea ice loss of moderate magnitude leads respectively to a negative or positive AO response in the large-scale tropospheric circulation (indicated in Figures 3a and 3c by the dark blue features), consistent with the stratospheric responses. However, for large-magnitude sea ice loss we find a similar strength of negative AO response in both cases (Figures 3b and 3d). This suggests that different spatial patterns of sea ice loss, when the loss is not too large in magnitude, can explain the contrasting tropospheric responses in previous studies. Furthermore, it implies that as the magnitude of sea ice loss increases, tropospheric mechanisms (which may tend to lead to a negative AO for both Atlantic and Pacific sector sea ice loss through, for example, reductions in meridional temperature gradient) become relatively more important than stratospheric mechanisms (which lead to oppositely signed AO responses)—compare the dotted arrows in Figures 3a and 3c with those in Figures 3b and 3d. This helps explain why different studies find tropospheric and stratospheric mechanisms to have different levels of importance (e.g., Nakamura, Yamazaki, Iwamoto, et al., 2016, find that stratospheric mechanisms are crucial in the response to recent sea ice loss, while Wu and Smith (2016) find that tropospheric and stratospheric mechanisms are equally important for late 21st century sea ice loss). SDT15's Pacific experiment also suggests that tropospheric mechanisms are more important for large-magnitude sea ice loss, since they find a stronger polar vortex but no northward shift of the zonal mean tropospheric eddy-driven jet.

However, within the current experimental setup we cannot definitively quantify the role stratospheric and tropospheric mechanisms played in the tropospheric AO responses. In future work we hope to address this by conducting additional experiments designed to isolate the role of the stratosphere (e.g., Hitchcock & Simpson, 2014). This will also help us understand sources of nonlinearity in the responses (e.g., the tropospheric AO response may reverse in sign for double the magnitude of Pacific sea ice loss because the tropospheric pathway strengthens at a greater rate than the stratospheric pathway, or because the stratosphere has relatively less effect on the troposphere).

In answer to the third research question (What are the effects on midlatitude surface temperatures?), we find that while there is a negative tropospheric AO in response to large magnitudes of both Atlantic and Pacific sector sea ice loss, there are contrasting effects on midlatitude surface temperatures (compare Figures 3b and 3d). Specifically, in the Atlantic (Pacific) case AO-induced cooling is absent in Northern Europe (North America), and any cooling only occurs in North America (Northern Europe). We show that this can be understood by decomposing the temperature response into an indirect part induced by the large-scale indirect circulation (AO) response, and a residual direct part, which is demonstrated to be local to the loss region, and is partly explained by the direct circulation response. In the Atlantic (Pacific) case, the direct circulation response is consistent with warm advection over Northern Europe (North America), and the counteraction of AO-induced cooling there (indicated in Figures 3b and 3d by the warm advection symbol). Thus, in the Atlantic (Pacific) case any cooling only occurs in North America (Northern Europe). This decomposition of the temperature

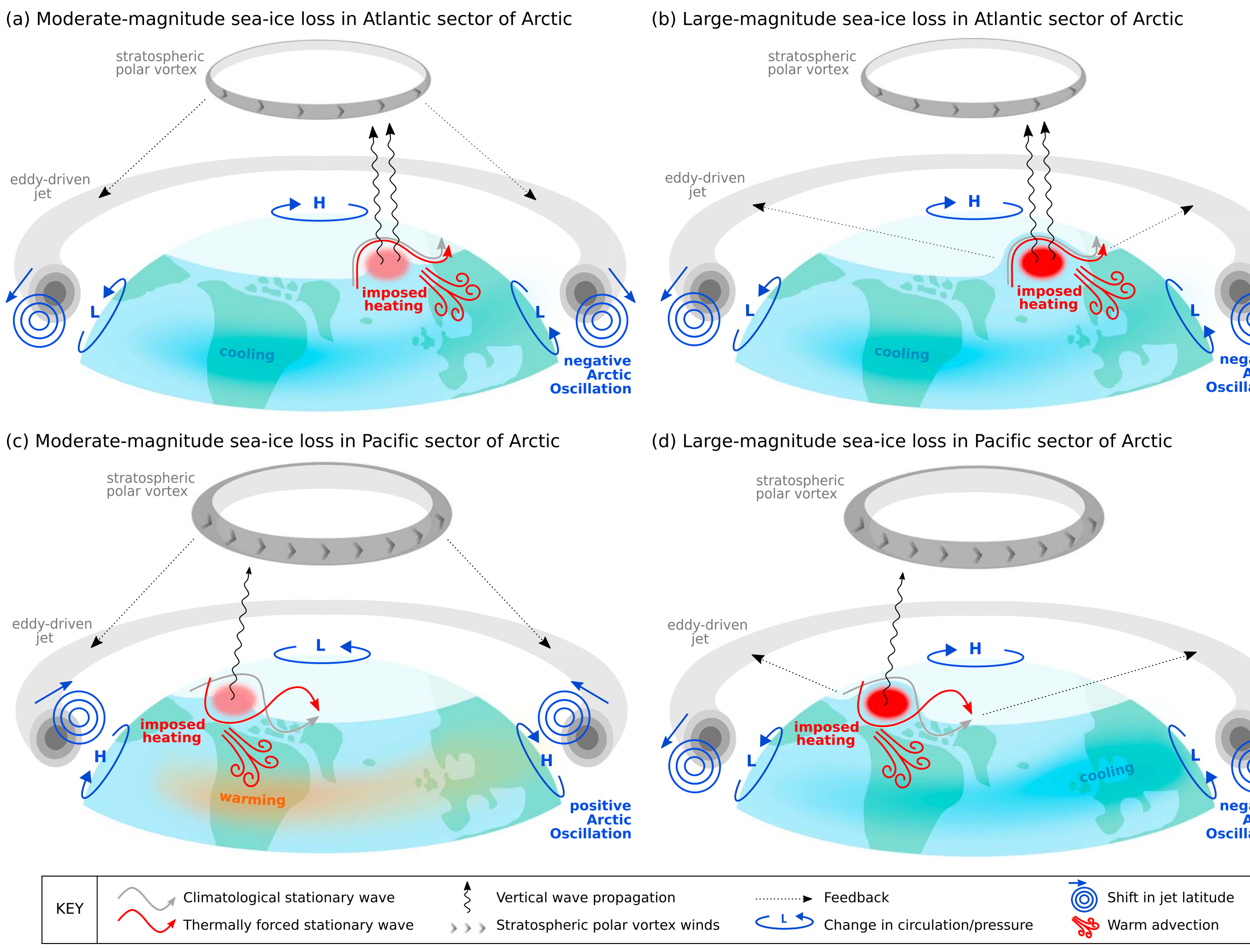

Figure 3. Schematic summarizing the key mechanisms that may link Arctic sea ice loss with changes in midlatitude surface temperatures, for different sectors and magnitudes of loss. (a, c) Moderate-magnitude and (b, d) large-magnitude (late 21st century) loss in the Atlantic or Pacific sector. Features of the direct/indirect response are shaded in red/dark blue.

response into direct and indirect parts is a new approach, but is similar in concept to the "thermodynamic" versus "dynamic" decomposition described by Screen et al. (2015) and others. However, we use the direct versus indirect terminology, since the direct temperature response involves both thermodynamic and dynamic processes. It also is similar in concept to Deser, Terray, et al.'s (2016) decomposition of air temperature trends into dynamical internal and forced components, and thermodynamic internal and forced components. Due to a lack of significance, our decomposition was not performed for the moderate-magnitude sea ice loss experiments. However, the temperature changes for moderate-magnitude Atlantic or Pacific sea ice loss are consistent with the AO responses and a direct warming effect local to the loss region (Figures 3a and 3c).

The temperature responses in the large-magnitude sea ice loss cases contrast with the observational study of Kug et al. (2015), who find that warming in the Barents-Kara (East Siberian-Chukchi) Seas is connected to wintertime cooling in Eurasia (North America). However, their results are for past warming, which is much smaller in magnitude than our anomalies. Therefore, the direct warming effect is likely not large enough to counteract the indirect cooling effect. Recent papers (e.g., McCusker et al., 2016) also show that recent wintertime Eurasian cooling can be explained entirely by natural variability.

The wider relevance of these results will now be considered. Since the spatial pattern and magnitude of future sea ice loss—and associated surface warming—is uncertain across climate models (Figure S1), they may indicate the range of potential atmospheric responses. For instance, for climate models with sea ice loss weighted toward the Atlantic sector (e.g., GISS), there could be a negative tropospheric AO and a cooler North America, regardless of the ice loss magnitude. However, for models with more Pacific sector sea ice loss and smaller/larger magnitudes of it (e.g., FIO-ESM/ACCESS), there could be a positive/negative AO and warmer midlatitudes/a cooler Northern Europe. Regarding models with ice loss equally weighted toward both sectors (e.g., HadGEM2), an additional 200 year long experiment with large-magnitude T_s anomalies imposed in the Atlantic and Pacific sectors simultaneously suggests that the sign of the response in the combined case is consistent with an addition of the responses in the separate cases (Figure S10). The combined case response is generally weaker than this addition suggests, however, as also found by Screen (2017a) but for a greater number of sea ice loss regions. The above scenarios put into context, for example, Screen's (2017b) finding that Northern European cooling is absent in the response to Arctic sea ice loss; this was only for sea ice loss that is equally weighted toward the Atlantic and Pacific sectors.

Acknowledgments
The authors would like to acknowledge helpful discussions with Peter Hitchcock, Alison Ming, Ted Shepherd, Maarten Ambaum, Doug Smith, and James Screen. Thank you also to Karen Smith and one anonymous reviewer for their valuable comments, which greatly helped to improve the manuscript. We acknowledge the World Climate Research Programme's Working Group on Coupled Modelling, which is responsible for CMIP, and we thank the climate modeling groups (listed in Table S1 of this paper) for producing and making available their model output. For CMIP the U.S. Department of Energy's Program for Climate Model Diagnosis and Intercomparison provides coordinating support and led development of software infrastructure in partnership with the Global Organization for Earth System Science Portals. We wish to thank STFC CEDA for use of the JASMIN storage and analysis platform, where the model experiment data are stored and analyzed. The data can be shared via this platform by contacting the author. This work was funded by a PhD studentship awarded to C.M.M. by the Cambridge Earth System Science NERC DTP (Natural Environment Research Council Doctoral Training Partnership).

References

Alexander, M. A., Bhatt, U. S., Walsh, J. E., Timlin, M. S., Miller, J. S., & Scott, J. D. (2004). The atmospheric response to realistic Arctic sea ice anomalies in an AGCM during winter. *Journal of Climate*, *17*, 890–905. https://doi.org/10.1175/1520-0442(2004)017<0890:TARTRA>2.0.CO;2

Ambaum, M. H. P., Hoskins, B. J., & Stephenson, D. B. (2001). Arctic oscillation or North Atlantic Oscillation? *Journal of Climate*, *14*, 3495–3507. https://doi.org/10.1175/1520-0442(2001)014<3495:AOONAO>2.0.CO;2

Baldwin, M. P., & Dunkerton, T. J. (2001). Stratospheric harbingers of anomalous weather regimes. *Science*, *294*, 581–584. https://doi.org/10.1126/science.1063315

Baldwin, M. P., Edmon, H. J., & Holton, J. R. (1985). A diagnostic study of eddy-mean flow interactions during FGGE SOP-1. *Journal of the Atmospheric Sciences*, *42*, 1838–1845. https://doi.org/10.1175/1520-0469(1985)042<1838:ADSOEM>2.0.CO;2

Boland, E. J. D., Bracegirdle, T. J., & Shuckburgh, E. F. (2016). Assessment of sea ice-atmosphere links in CMIP5 models. *Climate Dynamics*, *37*, 1–20. https://doi.org/10.1007/s00382-016-3367-1

Cai, D., Dameris, M., Garny, H., & Runde, T. (2012). Implications of all season Arctic sea-ice anomalies on the stratosphere. *Atmospheric Chemistry and Physics*, *12*, 11,819–11,831. https://doi.org/10.5194/acp-12-11819-2012

Cohen, J., Screen, J. A., Furtado, J. C., Barlow, M., Whittleston, D., Coumou, D., … Jones, J. (2014). Recent Arctic amplification and extreme mid-latitude weather. *Nature Geoscience*, *7*, 627–637. https://doi.org/10.1038/ngeo2234

Dee, D. P., Uppala, S. M., Simmons, A. J., Berrisford, P., Poli, P., Kobayashi, S., … Vitart, F. (2011). The ERA-Interim reanalysis: Configuration and performance of the data assimilation system. *Quarterly Journal of the Royal Meteorological Society*, *137*, 553–597. https://doi.org/10.1002/qj.828

Deser, C., Magnusdottir, G., Saravanan, R., & Phillips, A. (2004). The effects of North Atlantic SST and sea ice anomalies on the winter circulation in CCM3. Part II: Direct and indirect components of the response. *Journal of Climate*, *17*, 877–889. https://doi.org/10.1175/1520-0442(2004)017<0877:TEONAS>2.0.CO;2

Deser, C., Sun, L., Tomas, R. A., & Screen, J. (2016). Does ocean coupling matter for the northern extratropical response to projected Arctic sea ice loss? *Geophysical Research Letters*, *43*, 2149–2157. https://doi.org/10.1002/2016GL067792

Deser, C., Terray, L., & Phillips, A. S. (2016). Forced and internal components of winter air temperature trends over North America during the past 50 years: Mechanisms and implications. *Journal of Climate*, *29*, 2237–2258. https://doi.org/10.1175/JCLI-D-15-0304.1

García-Serrano, J., Frankignoul, C., Gastineau, G., & Cámara, A. (2015). On the predictability of the winter Euro-Atlantic climate: Lagged influence of autumn Arctic sea ice. *Journal of Climate*, *28*, 5195–5216. https://doi.org/10.1175/JCLI-D-14-00472.1

Guirguis, K., Gershunov, A., Schwartz, R., & Bennett, S. (2011). Recent warm and cold daily winter temperature extremes in the Northern Hemisphere. *Geophysical Research Letters*, *38*, L17701. https://doi.org/10.1029/2011GL048762

Hitchcock, P., & Simpson, I. R. (2014). The downward influence of stratospheric sudden warmings. *Journal of the Atmospheric Sciences*, *71*, 3856–3876. https://doi.org/10.1175/JAS-D-14-0012.1

Honda, M., Inoue, J., & Yamane, S. (2009). Influence of low Arctic sea-ice minima on anomalously cold Eurasian winters. *Geophysical Research Letters*, *36*, L08707. https://doi.org/10.1029/2008GL037079

Hoskins, B. J., & Karoly, D. J. (1981). The steady linear response of a spherical atmosphere to thermal and orographic forcing. *Journal of Atmospheric Science*, *38*, 1179–1196. https://doi.org/10.1175/1520-0469(1981)038<1179:TSLROA>2.0.CO;2

Joshi, M., Stringer, M., Wiel, K., O'Callaghan, A., & Fueglistaler, S. (2015). IGCM4: A fast, parallel and flexible intermediate climate model. *Geoscientific Model Development*, *8*, 1157–1167. https://doi.org/10.5194/gmd-8-1157-2015

Kim, B.-M., Son, S.-W., Min, S.-K., Jeong, J.-H., Kim, S.-J., Zhang, X., … Yoon, J.-H. (2014). Weakening of the stratospheric polar vortex by Arctic sea-ice loss. *Nature Communications*, *5*, 4646. https://doi.org/10.1038/ncomms5646

King, M. P., Hell, M., & Keenlyside, N. (2016). Investigation of the atmospheric mechanisms related to the autumn sea ice and winter circulation link in the Northern Hemisphere. *Climate Dynamics*, *46*, 1185–1195. https://doi.org/10.1007/s00382-015-2639-5

Koenigk, T., Caian, M., Nikulin, G., & Schimanke, S. (2016). Regional Arctic sea ice variations as predictor for winter climate conditions. *Climate Dynamics*, *46*, 317–337. https://doi.org/10.1007/s00382-015-2586-1

Kug, J.-S., Jeong, J.-H., Jang, Y.-S., Kim, B.-M., Folland, C. K., Min, S.-K., & Son, S.-W. (2015). Two distinct influences of Arctic warming on cold winters over North America and East Asia. *Nature Geoscience*, *8*, 759–762. https://doi.org/10.1038/ngeo2517

McCusker, K. E., Fyfe, J. C., & Sigmond, M. (2016). Twenty-five winters of unexpected Eurasian cooling unlikely due to Arctic sea-ice loss. *Nature Geoscience*, *9*(11), 838–842. https://doi.org/10.1038/ngeo2820

Mori, M., Watanabe, M., Shiogama, H., Inoue, J., & Kimoto, M. (2014). Robust Arctic sea-ice influence on the frequent Eurasian cold winters in past decades. *Nature Geoscience*, *7*, 869–873. https://doi.org/10.1038/ngeo2277

Nakamura, T., Yamazaki, K., Iwamoto, K., Honda, M., Miyoshi, Y., Ogawa, Y., & Ukita, J. (2015). A negative phase shift of the winter AO/NAO due to the recent Arctic sea-ice reduction in late autumn. *Journal of Geophysical Research: Atmospheres*, *120*, 3209–3227. https://doi.org/10.1002/2014JD022848

Nakamura, T., Yamazaki, K., Honda, M., Ukita, J., Jaiser, R., Handorf, D., & Dethloff, K. (2016). On the atmospheric response experiment to a Blue Arctic Ocean. *Geophysical Research Letters*, *43*, 10,394–10,402. https://doi.org/10.1002/2016GL070526

Nakamura, T., Yamazaki, K., Iwamoto, K., Honda, M., Miyoshi, Y., Ogawa, Y., … Ukita, J. (2016). The stratospheric pathway for Arctic impacts on midlatitude climate. *Geophysical Research Letters*, *43*, 3494–3501. https://doi.org/10.1002/2016GL068330

National Snow and Ice Data Center (2016). Arctic sea ice news and analysis: Yearly archives: 2016. Retrieved from http://nsidc.org/arcticseaicenews/2016/

Nishii, K., Nakamura, H., & Miyasaka, T. (2009). Modulations in the planetary wave field induced by upward-propagating Rossby wave packets prior to stratospheric sudden warming events: A case-study. *Quarterly Journal of the Royal Meteorological Society*, *135*, 36–51. https://doi.org/10.1002/qj.359

O'Callaghan, A., Joshi, M., Stevens, D., & Mitchell, D. (2014). The effects of different sudden stratospheric warming type on the ocean. *Geophysical Research Letters*, *41*, 7739–7745. https://doi.org/10.1002/2014GL062179

Orsolini, Y. J., Senan, R., Benestad, R. E., & Melsom, A. (2012). Autumn atmospheric response to the 2007 low Arctic sea ice extent in coupled ocean-atmosphere hindcasts. *Climate Dynamics*, *38*, 2437–2448. https://doi.org/10.1007/s00382-011-1169-z

Osborn, T. J. (2011). Winter 2009/2010 temperatures and a recordbreaking North Atlantic Oscillation index. *Weather*, *66*, 19–21. https://doi.org/10.1002/wea.660

Overland, J. E., Dethloff, K., Francis, J. A., Hall, R. J., Hanna, E., Kim, S. J., … Vihma, T. (2016). Nonlinear response of mid-latitude weather to the changing Arctic. *Nature Climate Change*, *6*, 992–999. https://doi.org/10.1038/nclimate3121

Palmer, T. N. (1981). Diagnostic study of a wavenumber-2 stratospheric sudden warming in a transformed Eulerian-mean formalism. *Journal of the Atmospheric Sciences*, *38*, 844–855. https://doi.org/10.1175/1520-0469(1981)038<0844:DSOAWS>2.0.CO;2

Pedersen, R. A., Cvijanovic, I., Langen, P. L., & Vinther, B. M. (2016). The impact of regional Arctic sea ice loss on atmospheric circulation and the NAO. *Journal of Climate*, *29*, 889–902. https://doi.org/10.1175/JCLI-D-15-0315.1

Peings, Y., & Magnusdottir, G. (2014). Response of the wintertime Northern Hemisphere atmospheric circulation to current and projected Arctic sea-ice decline: A numerical study with CAM5. *Journal of Climate*, *27*, 244–264. https://doi.org/10.1175/JCLI-D-13-00272.1

Petoukhov, V., & Semenov, V. A. (2010). A link between reduced Barents-Kara sea ice and cold winter extremes over northern continents. *Journal of Geophysical Research*, *115*, D21111. https://doi.org/10.1029/2009JD013568

Scinocca, J. F., Reader, M. C., Plummer, D. A., Sigmond, M., Kushner, P. J., Shepherd, T. G., & Ravishankara, R. (2009). Impact of sudden Arctic sea-ice loss on stratospheric polar ozone recovery. *Geophysical Research Letters*, *36*, L24701. https://doi.org/10.1029/2009GL041239

Screen, J. A. (2017a). Simulated atmospheric response to regional and pan-Arctic sea ice loss. *Journal of Climate*, *30*, 3945–3962. https://doi.org/10.1175/JCLI-D-16-0197.1

Screen, J. A. (2017b). The missing Northern European winter cooling response to Arctic sea ice loss. *Nature Communications*, *8*, 14603. https://doi.org/10.1038/ncomms14603

Screen, J. A., & Simmonds, I. (2010). The central role of diminishing sea ice in recent Arctic temperature amplification. *Nature*, *464*, 1334–1337. https://doi.org/10.1038/nature09051

Screen, J. A., Simmonds, I., Deser, C., & Tomas, R. (2013). The atmospheric response to three decades of observed Arctic sea ice loss. *Journal of Climate*, *26*, 1230–1248. https://doi.org/10.1175/JCLI-D-12-00063.1

Screen, J. A., Deser, C., Simmonds, I., & Tomas, R. (2014). Atmospheric impacts of Arctic sea-ice loss, 1979–2009: Separating forced change from atmospheric internal variability. *Climate Dynamics*, *43*, 333–344. https://doi.org/10.1007/s00382-013-1830-9

Screen, J. A., Deser, C., & Sun, L. (2015). Reduced risk of North American cold extremes due to continued Arctic sea ice loss. *Bulletin of the American Meteorological Society*, *96*, 1489–1503. https://doi.org/10.1175/BAMS-D-14-00185.1

Seierstad, I. A., & Bader, J. (2009). Impact of a projected future Arctic sea ice reduction on extratropical storminess and the NAO. *Climate Dynamics*, *33*, 937–943. https://doi.org/10.1007/s00382-008-0463-x

Singarayer, J. S., Bamber, J. L., & Valdes, P. J. (2006). Twenty-first-century climate impacts from a declining Arctic sea ice cover. *Journal of Climate*, *19*, 1109–1125. https://doi.org/10.1175/JCLI3649.1

Smith, K. L., Fletcher, C. G., & Kushner, P. J. (2010). The role of linear interference in the annular mode response to extratropical surface forcing. *Journal of Climate*, *23*, 6036–6050. https://doi.org/10.1175/2010JCLI3606.1

Sun, L., Deser, C., Polvani, L. M., & Tomas, R. (2014). Influence of projected Arctic sea ice loss on polar stratospheric ozone and circulation in spring. *Environmental Research Letters*, *9*, 084016. https://doi.org/10.1088/1748-9326/9/8/084016

Sun, L., Deser, C., & Tomas, R. A. (2015). Mechanisms of stratospheric and tropospheric circulation response to projected Arctic sea ice loss. *Journal of Climate*, *28*, 7824–7845. https://doi.org/10.1175/JCLI-D-15-0169.1

Taylor, K. E., Stouffer, R. J., & Meehl, G. A. (2012). An overview of CMIP5 and the experiment design. *Bulletin of the American Meteorological Society*, *93*, 485–498. https://doi.org/10.1175/bams-d-11-00094.1

Van Oldenborgh, G. J., Haarsma, R., De Vries, H., & Allen, M. R. (2015). Cold extremes in North America vs. mild weather in Europe: The winter of 2013–14 in the context of a warming world. *Bulletin of the American Meteorological Society*, *96*, 707–714. https://doi.org/10.1175/BAMS-D-14-00036.1

Wu, Y., & Smith, K. L. (2016). Response of Northern Hemisphere midlatitude circulation to Arctic amplification in a simple atmospheric general circulation model. *Journal of Climate*, *29*, 2041–2058. https://doi.org/10.1175/JCLI-D-15-0602.1